

Single-gap Isotropic s -wave Superconductivity in Single Crystals AuSn_4

Sunil Ghimire^{1,2}, Kamal R. Joshi^{1,2}, Elizabeth H. Krenkel^{1,2}, Makariy A. Tanatar^{1,2},
Marcin Kończykowski³, Romain Grasset³, Paul C. Canfield^{1,2} and Ruslan Prozorov^{1,2*}

¹ Ames National Laboratory, Ames, Iowa 50011, USA

² Department of Physics & Astronomy, Iowa State University, Ames, Iowa 50011, USA

³ Laboratoire des Solides Irradiés, CEA/DRF/IRAMIS, École Polytechnique, CNRS, Institut Polytechnique de Paris, F-91128 Palaiseau, France

* prozorov@ameslab.gov

Abstract

London, $\lambda_L(T)$, and Campbell, $\lambda_C(T)$, penetration depths were measured in single crystals of a topological superconductor candidate AuSn_4 . At low temperatures, $\lambda_L(T)$ is exponentially attenuated and, if fitted with the power law, $\lambda(T) \sim T^n$, gives exponents $n > 4$, indistinguishable from the isotropic single s -wave gap Bardeen-Cooper-Schrieffer (BCS) asymptotic. The superfluid density fits perfectly in the entire temperature range to the BCS theory. The superconducting transition temperature, $T_c = 2.40 \pm 0.05$ K, does not change after 2.5 MeV electron irradiation, indicating the validity of the Anderson theorem for isotropic s -wave superconductors. Campbell penetration depth before and after electron irradiation shows no hysteresis between the zero-field cooling (ZFC) and field cooling (FC) protocols, consistent with the parabolic pinning potential. Interestingly, the critical current density estimated from the original Campbell theory decreases after irradiation, implying that a more sophisticated theory involving collective effects is needed to describe vortex pinning in this system. In general, our thermodynamic measurements strongly suggest that the bulk response of the AuSn_4 crystals is fully consistent with the isotropic s -wave weak-coupling BCS superconductivity.

Copyright attribution to authors.

This work is a submission to SciPost Physics.

License information to appear upon publication.

Publication information to appear upon publication.

Received Date

Accepted Date

Published Date

1

2 Contents

3	1 Introduction	2
4	2 Samples and Methods	2
5	3 Results	3
6	3.1 London penetration depth	3
7	3.2 Campbell penetration depth	6
8	4 Conclusions	8
9	5 Acknowledgements	8

11

12

13 **1 Introduction**

14 In recent years, superconductors with topological features in their electronic bandstructure
15 have attracted significant interest for various novel features predicted by a well-developed
16 theory. For example, emerging zero-energy excitations called Majorana fermions [1]. On the
17 material side, the search for topological superconductors (TSCs) is very active but so far has
18 yielded only a few “candidates” whose topological properties have not yet been fully confirmed
19 experimentally, including UTe_2 [2], Sr_2RuO_4 [3–5], UPt_3 [6], 2M-WS_2 [7], and $\text{M}_x\text{Bi}_2\text{Se}_3$
20 with $\text{M}=\text{Cu}$ [8, 9]. The subject of this study, AuSn_4 , is another promising TSC candidate with
21 theoretically predicted non-trivial topological characteristics [10–13].

22 The superconductivity in orthorhombic AuSn_4 with a transition temperature to the super-
23 conducting state, $T_c = 2.4$ K, was discovered in 1962 [14]. This compound is isostructural
24 to PtSn_4 [15] and PdSn_4 [16], which are not superconductors. The first principal study sug-
25 gests semimetallic behavior with type I nodes [12]. The magneto-transport measurements
26 show two-dimensional (2D) superconductivity in AuSn_4 [11, 17]. Recently, ARPES measure-
27 ments supported by DFT calculations [13] revealed nearly degenerate polytypes in AuSn_4
28 crystals, making it a unique case of a three-dimensional (3D) electronic band structure with
29 properties of a low-dimensional layered material. Thermodynamic magnetization and spe-
30 cific heat measurement in AuSn_4 single crystals are consistent with conventional nodeless
31 s -wave Bardeen-Cooper-Schrieffer (BCS) [18, 19] superconductivity [11]. Scanning tunnel-
32 ing microscopy (STM) measurements determined the superconducting gap to T_c ratio close
33 to the s -wave BCS value of $\Delta/T_c = 1.76$ [13]. However, other STM measurements suggest
34 unconventional 2D superconductivity with a mixture of p -wave surface states and s -wave
35 bulk [10]. Clearly, more measurements are required for an objective and conclusive determi-
36 nation of the nature of superconductivity in AuSn_4 .

37 Here, we probe the bulk nature of superconductivity in AuSn_4 single crystals by measur-
38 ing London and Campbell penetration depths using a highly sensitive tunnel-diode resonator
39 (TDR). Furthermore, we examine the response to a controlled non-magnetic point-like disorder
40 induced by 2.5 MeV electron irradiation. We conclude that AuSn_4 is a robust isotropic
41 s -wave superconductor in the bulk. However, we cannot exclude the possibility that it could
42 have a different type of superconductivity in the surface atomic layers, where the STM is most
43 sensitive.

44 **2 Samples and Methods**

45 Single crystals of AuSn_4 were grown with excess Sn flux [13, 20, 21]. High-purity Au and Sn
46 were mixed in a 12:88 ratio in a fritted crucible and sealed in a quartz ampoule under an Ar
47 gas atmosphere. The ampoule was heated to 1100 °C over 12 hours, then cooled to 250 °C
48 in 12 hours, and significantly slower to 230 °C over 90 hours. The ampoule was held at this
49 temperature for 48 hours prior to removal from the furnace.

50 The London penetration depth, $\lambda(T)$, was measured using a sensitive frequency-domain
51 self-oscillating tunnel-diode resonator (TDR) operating at a frequency of around 14 MHz. The
52 measurements were performed in a cryostat ^3He with a base temperature of ≈ 400 mK, which

53 is $0.17T_c$, allowing us to examine the low-temperature limit, which starts below approximately
 54 $T_c/3$, where the superconducting gap is approximately constant. The experimental setup,
 55 measurement protocols, and calibration are described in detail elsewhere [22–26]. In the
 56 experiment, the variation, $\Delta\lambda(T) = \lambda(T) - \lambda(0.4\text{K})$, is extracted from the resonant frequency
 57 shift. The small excitation magnetic field of 20 Oe ensures a true Campbell regime when
 58 vortices are gently perturbed. For TDR measurements, the samples were cut into cuboids that
 59 are typically of size $0.6 \times 0.4 \times 0.1 \text{ mm}^3$.

60 Point-like disorder was introduced at the SIRIUS facility in the Laboratoire des Solides
 61 Irradiés at École Polytechnique in Palaiseau, France. Electrons, accelerated in a pelletron-
 62 type linear accelerator to 2.5 MeV, knock out ions, creating vacancy-interstitial Frenkel pairs
 63 [27, 28]. During irradiation, the sample is immersed in liquid hydrogen at around 20 K. This
 64 ensures efficient heat removal upon impact and prevents immediate recombination and mi-
 65 gration of the produced atomic defects. The acquired irradiation dose is determined by mea-
 66 suring the total charge collected by a Faraday cage located behind the sample. As such, the
 67 acquired dose is measured in the “natural” units of C/cm^2 , which is equal to $1 \text{ C}/\text{cm}^2 \equiv 1/e \approx$
 68 6.24×10^{18} electrons per cm^2 . Upon warming to room temperature, some defects recom-
 69 bine, and some migrate to various sinks (dislocations, surfaces, etc.). This leaves a metastable
 70 population, about 70%, of point-like defects [29, 30]. Importantly, the same sample has been
 71 measured before and after electron irradiation.

72 3 Results

73 3.1 London penetration depth

74 Figure 1 shows the low-temperature dependence of the change in the London penetration
 75 depth, $\Delta\lambda(T) = \lambda(T) - \lambda(T_{min} = 0.4 \text{ K})$ before (blue circles) and after $2.5 \text{ C}/\text{cm}^2$ electron
 76 irradiation (red circles). The upper left inset shows the exponent n determined from the
 77 power-law fitting, $\Delta\lambda(T) \sim At^n$, as a function of the upper fitting limit, $t_{max} = T_{max}/T_c$. The
 78 solid lines in the main frame show an example of such a fitting with $t_{max} = 0.4$. The results
 79 show a robust and consistent behavior with $n \geq 4$, indicating experimentally indistinguishable
 80 from the exponential temperature dependence. The exponent, n , decreased after irradiation
 81 as it should be in an s -wave superconductor [31, 32].

82 The upper right inset of Fig.1 shows $\Delta\lambda(T)$ of the same sample in its pristine state and after
 83 $2.15 \text{ C}/\text{cm}^2$ electron irradiation as a function of absolute temperature T . One might think that
 84 for some reason (e.g., defect annealing and recombination), there was no increase in disorder
 85 after irradiation. This is not the case, as the saturation value above T_c increased substantially.
 86 The saturation is determined by the skin depth in the normal state, $\delta_{skin} = \sqrt{\rho/\mu_0\pi f}$, where
 87 $\mu_0 = 4\pi \times 10^{-7} \text{ H/m}$ is the vacuum permeability, and ρ is the resistance. We did not measure
 88 resistivity in this AuSn_4 sample, but we directly compared resistivity from transport measure-
 89 ments and extracted from the skin depth on the same samples in other compounds and always
 90 found good quantitative agreement [33, 34]. The upper critical fields are small, $H_{c2}^{\parallel ab} = 130 \text{ Oe}$
 91 and $H_{c2}^{\parallel c} = 90 \text{ Oe}$ [11]. Combined with the trend of measured magnetoresistance [13], the ex-
 92 pected variation above T_c is negligible. An increase in δ_{skin} at a fixed frequency, f , is due to an
 93 increase in resistivity, which is indicative of the increased scattering. Therefore, the fact that
 94 the superconducting transition T_c remains unchanged is consistent with the Anderson theorem
 95 for isotropic s -wave superconductors [35, 36]. We observe similar robust superconductivity
 96 in another low- T_c superconductor with non-trivial topology, LaNiGa_2 [37].

97 The exponential temperature dependence of $\lambda(T)$ can be fitted with the well-known low-
 98 temperature asymptotic BCS, $\Delta\lambda(T) = \lambda(0)\sqrt{\frac{\pi\delta}{2t}}e^{-\frac{\delta}{t}}$ [19], where the ratio $\delta = \Delta(0)/T_c$

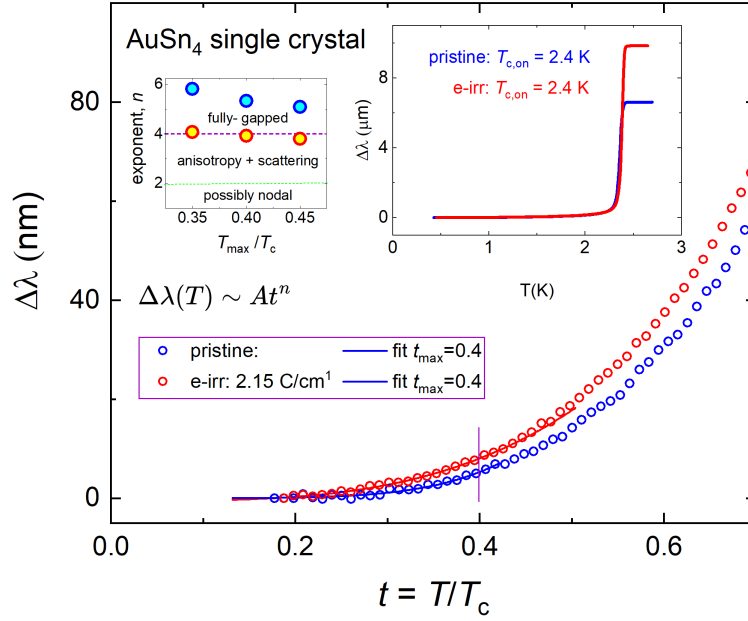


Figure 1: Main Panel: Low-temperature temperature variation of the London penetration depth $\Delta\lambda(T) = \lambda(T) - \lambda(0.4 \text{ K})$ as a function of normalized temperature, $t = T/T_c$, for pristine (blue circles) and irradiated at 2.5 C/cm^2 (red circles) single crystal of AuSn_4 . Lines show fits to the power law, $\Delta\lambda(T) \sim At^n$, with the upper range of $t_{\text{max}} = 0.4$. The top right inset shows the $\Delta\lambda(T)$ in the whole temperature range, showing sharp superconducting transition with onset $T_c = 2.4 \text{ K}$ for both pristine and electron irradiated state. The top left inset shows the exponent n versus the upper limit of the power-law fitting, $t_{\text{max}} = T_{\text{max}}/T_c$, indicating robustness of the power law, experimentally indistinguishable from exponential.

99 was fixed at $\delta \approx 1.76$, leaving only one free parameter $\lambda(0)$. The fitting is shown in the
 100 top panel of Fig.2. It produces $\lambda(0) = 150 \text{ nm}$ in the pristine state (blue fitting curve and
 101 blue data symbols) and $\lambda(0) = 258 \text{ nm}$ after 2.15 C/cm^2 electron irradiation (red curve and
 102 symbols). With these numbers, we can calculate the superfluid density in the full tempera-
 103 ture range using $\rho_s(T) \equiv (\lambda(0)/\lambda(T))^2 = (1 + \Delta\lambda(T)/\lambda(0))^{-2}$. The bottom panel of Fig.2
 104 shows $\rho_s(T)$ by blue and red circles for the pristine and irradiated states of the same sam-
 105 ple, respectively. The theoretical lines of the clean (blue) and dirty (red) limits were cal-
 106 culated self-consistently using the Eilenberger formalism [39]. We note that the analytical
 107 dirty limit formula, $\rho_s = (\Delta(T)/\Delta(0)) \tanh(\Delta(T)/2T)$ reproduces the numerical calcula-
 108 tion precisely [38]. Examining Fig.2 we conclude that the classical BCS theory describes the
 109 experimental data well.

110 To summarize our findings from measurements of the London penetration depth, $\lambda(T)$,
 111 several independent parameters: (1) low-temperature behavior of $\lambda(T)$; (2) full temperature
 112 range behavior of ρ_s ; (3) disorder-independent T_c before and after electron irradiation, fully
 113 agree with the BCS theory for the isotropic s -wave gap with the ratio $\delta = \Delta(0)/T_c \approx 1.76$.
 114 This is the nature of superconductivity in the bulk of AuSn_4 crystals. However, our measure-
 115 ments would not pick up a tiny signal coming from the surface atomic layers, so unconventional
 116 topological features are still possible.

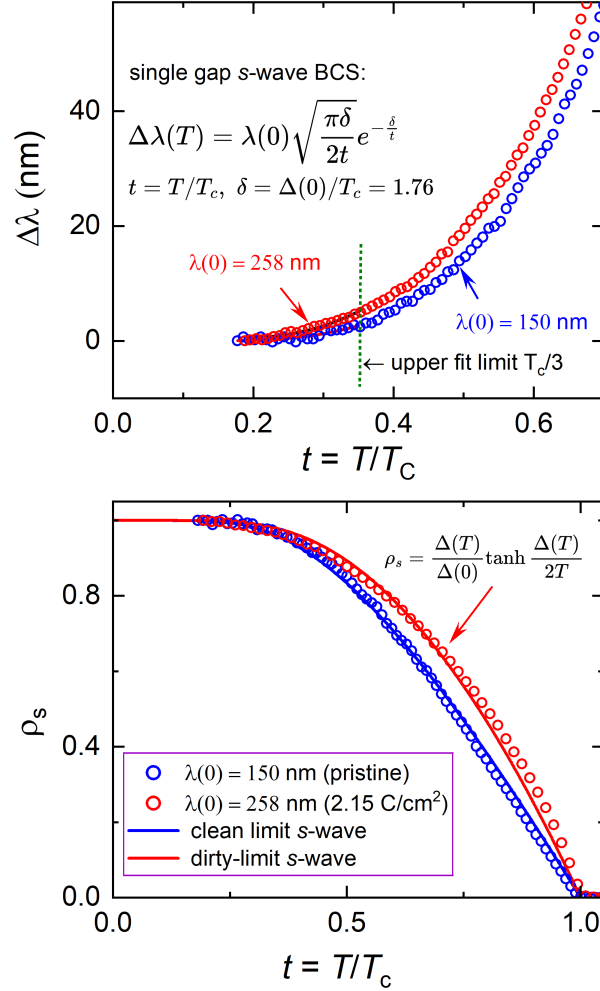


Figure 2: Top panel. Fit to the BCS low-temperature asymptotic, $\Delta\lambda(T) = \lambda(0) \sqrt{\frac{\pi\delta}{2t}} e^{-\frac{\delta}{t}}$ with a fixed ratio $\delta = \Delta(0)/T_c \approx 1.76$ leaving only one free parameter, $\lambda(0) = 150 \text{ nm}$ in the pristine sample (blue fitting curve and blue data symbols) and $\lambda(0) = 258 \text{ nm}$ after 2.15 C/cm^2 electron irradiation (red curve and symbols). Bottom panel: Superfluid density calculated from the data, $\rho_s(T) = (1 + \Delta\lambda(T)/\lambda(0))^{-2}$. Solid lines show self-consistent full temperature range calculations using Eilenberger formalism for pristine (blue line) and irradiated (red line) states. The known analytical expression for the s-wave dirty limit is shown in [38].

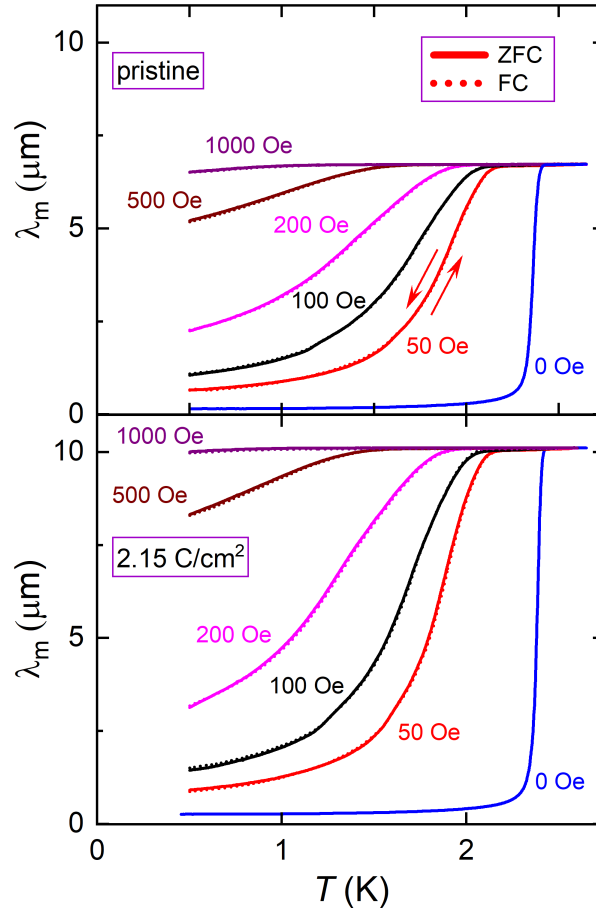


Figure 3: Temperature variation of the measured magnetic penetration depth, λ_m , before (top panel) and after (bottom panel) electron irradiation, measured with the various dc magnetic fields applied along the c -axis. The field values are shown. Solid lines correspond to zero-field cooling (ZFC), and dotted lines correspond to field cooling (FC) protocols. For one curve, this is shown by arrows. The ZFC and FC curves are indistinguishable, implying that the process is completely reversible, indicating the pinning potential's parabolic shape. Note that the axes scales are the same in the top and bottom panels, aiding in a visual comparison of the effect of irradiation.

117 3.2 Campbell penetration depth

118 The temperature variation of the magnetic penetration depth before (top panel) and after (bot-
 119 tom panel) electron irradiation, measured in various dc magnetic fields applied along the c -
 120 axis, is shown in Fig.3. The field values are shown next to each curve. Solid lines correspond
 121 to zero-field cooling (ZFC) in all curves, and dotted lines correspond to field cooling (FC) pro-
 122 tocols. For one curve, this is shown by arrows. The ZFC and FC curves are indistinguishable,
 123 implying that the process is totally reversible, which indicates a parabolic shape of the pinning
 124 potential.

125 In the presence of an external DC magnetic field, Abrikosov vortices penetrate the sample
 126 and form a vortex lattice. Then the measured penetration depth, λ_m , has two contributions,
 127 the usual London penetration depth that in this section we explicitly denote as λ_L , and the
 128 Campbell penetration depth λ_C , which is a characteristic length scale over which a small ac
 129 perturbation is transmitted elastically by a vortex lattice into the sample [40–43]. More specif-

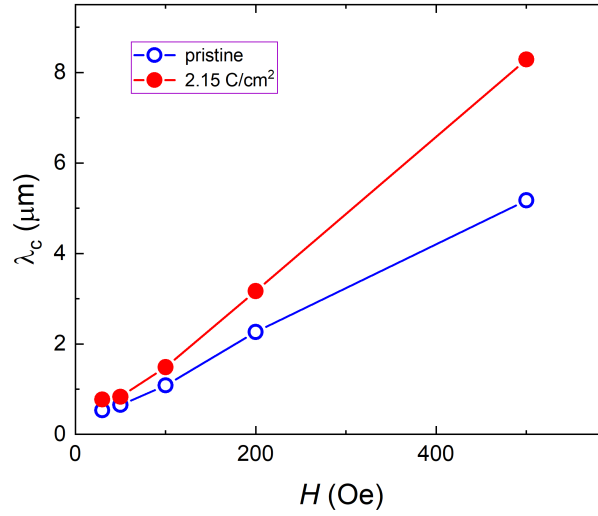


Figure 4: Campbell penetration depth, $\lambda_c^2 = \sqrt{\lambda_m^2 - \lambda_L^2}$ as a function of an applied magnetic field, H , evaluated from the data shown in Fig. 3 at a fixed temperature of $T = 0.5$ K. for a FC protocol comparing pristine (blue symbols) and irradiated (red symbols) states of the same sample.

130 ically, the amplitude of the ac perturbation must be small enough so that the vortices remain
 131 in their potential well, and their motion is described by the reversible linear elastic response.
 132 In this case, $\lambda_m^2 = \lambda_L^2 + \lambda_c^2$ [44, 45]. This requirement of a very small amplitude makes most
 133 conventional ac susceptibility techniques inapplicable for the measurements of the Campbell
 134 length. Specialized frequency domain resonators with sufficient sensitivity to a small excita-
 135 tion ac magnetic field are needed [46, 47]. Until now, only a few experimental studies have
 136 been published [46–50].

137 Figure 3 shows the temperature-dependent variation of the magnetic penetration depth,
 138 $\lambda_m(T) = \lambda_L(0) + \Delta\lambda_m(T)$, for different values of the dc magnetic field applied parallel to
 139 the sample c -axis. For $\lambda_L(0)$, we have used the values obtained from the BCS fit; see the
 140 upper panel of Fig. 2. Then, we assumed that, above T_c , the resistivity is field independent,
 141 so we adjusted other curves to match that value. The top panel shows a pristine state, and the
 142 bottom panel shows the same sample after electron irradiation.

143 Generally speaking, the Campbell penetration depth can exhibit a hysteresis upon warm-
 144 ing and cooling, indicating an anharmonic (non-parabolic) pinning potential and/or strong
 145 pinning [43, 46, 50, 51]. Therefore, there are two types of measurement protocols: zero-field
 146 cooling (ZFC) and field cooling (FC). In the ZFC protocol, the Campbell length is measured
 147 on warming after the sample was cooled in a zero magnetic field and the target field was ap-
 148 plied at the base temperature (solid lines in Fig. 3). In the FC protocol, measurements are
 149 performed on cooling in a target magnetic field applied above T_c (dotted lines in Fig. 3). For
 150 both pristine and irradiated states, $\lambda_m(T)$ shows a monotonic increase with temperature, and
 151 there is no hysteresis between the ZFC and FC protocols. To aid in visualizing the effect of
 152 irradiation, the scales of the axes in Fig. 3 are the same in the top and bottom panels. It is
 153 clear that the measured penetration depth has increased after electron irradiation.

154 Figure 4 shows the Campbell penetration depth as a function of an applied magnetic field,
 155 H , evaluated from the data shown in Fig. 3 at a fixed temperature of $T = 0.5$ K for a FC protocol
 156 comparing pristine (blue symbols) and irradiated (red symbols) states of the same sample.
 157 The Campbell length λ_c increases after irradiation. In the simple Campbell model [40, 41],
 158 $\lambda_c^2 = \phi_0 H / \alpha$, where ϕ_0 is the magnetic flux quantum and α is the curvature of the pinning
 159 potential, $\alpha = d^2U/dr^2$. The critical current density $j_c = \alpha r_p / \phi_0 = H r_p / \lambda_c^2$, where r_p

160 is the radius of the pinning potential, usually assumed to be the coherence length, ξ . We
 161 note that this critical current is not the same as the persistent current in other magnetization
 162 measurements because of magnetic relaxation. With an operational frequency of 14 MHz,
 163 unattainable in conventional ac susceptometry, our estimate of the critical current density is
 164 much closer to the true critical value. The dc magnetization gives an even lower current density
 165 as a result of a long time window of data acquisition.

166 In a more general picture, α is determined by the elementary pinning forces [42, 43, 52].
 167 In the original model with a fixed r_p , the Campbell length is expected to scale as $\lambda_C \sim \sqrt{H}$,
 168 but Fig. 4 shows a practically linear temperature dependence, especially after irradiation. This
 169 indicates that vortex pinning in AuSn₄ is more complicated with a field-dependent radius of
 170 the pinning potential, which is possible, for example, in a collective pinning theory when the
 171 vortex lattice evolves from the single-vortex pinning regime to the vortex bundle regime [53].
 172 In addition, it is known that the coherence length increases with the magnetic field [54].
 173 Therefore, if $\xi \sim H$, then λ_C will be a linear function of the applied field. As for the difference
 174 between pristine and irradiated states, it is possible that the collective pinning in the pristine
 175 state is replaced by the disordered vortex phase after electron irradiation, and one cannot
 176 directly compare the critical current densities using the same formula. In any case, the nature
 177 of pinning in AuSn₄ requires further investigation.

178 4 Conclusions

179 We report measurements of London, $\lambda_L(T)$, and Campbell, $\lambda_C(T)$, penetration depths in single
 180 crystals of the topological superconductor candidate AuSn₄ to elucidate the nature of super-
 181 conductivity in the bulk. Several independent parameters studied before and after 2.5 MeV
 182 electron irradiation unambiguously point to isotropic single *s*-wave gap weak coupling BCS
 183 superconductor. Specifically, the superfluid density before and after electron irradiation over-
 184 laps almost perfectly with the parameter-free theoretical BCS curves in the full temperature
 185 range for clean and dirty limits, respectively. The Campbell penetration depth before and af-
 186 ter electron irradiation does not show hysteresis between the ZFC and FC data, indicating a
 187 parabolic shape of the pinning potential. However, the *H*-linear behavior of λ_C implies either
 188 the field-dependent Labusch parameter, α , or the radius of the pinning potential, r_p , or both.
 189 Considering the low pinning in AuSn₄ single crystals and the point-like nature of the induced
 190 defects, such a field dependence may be expected in the vortex bundle regimes within the
 191 collective pinning theory [53].

192 5 Acknowledgements

193 We thank Hermann Suderow for fruitful discussions.

194 **Funding information:** This work was supported by the US DOE, Office of Science, BES Materi-
 195 als Science and Engineering Division under the contract # DE-AC02-07CH11358. The authors
 196 acknowledge support from the EMIRA French network (FR CNRS 3618) on the SIRIUS plat-
 197 form.

198 References

- 199 [1] C. Nayak, S. H. Simon, A. Stern, M. Freedman and S. D. Sarma, *Non-abelian anyons*
 200 *and topological quantum computation*, *Reviews of Modern Physics* **80**(3), 1083 (2008),

- 201 doi:[10.1103/RevModPhys.80.1083](https://doi.org/10.1103/RevModPhys.80.1083).
- 202 [2] S. Ran, C. Eckberg, Q.-P. Ding, Y. Furukawa, T. Metz, S. R. Saha, I.-L. Liu, M. Zic, H. Kim,
203 J. Paglione *et al.*, *Nearly ferromagnetic spin-triplet superconductivity*, *Science* **365**(6454),
204 684 (2019), doi:[10.1126/science.aav8645](https://doi.org/10.1126/science.aav8645).
- 205 [3] Y. Maeno, S. Kittaka, T. Nomura, S. Yonezawa and K. Ishida, *Evaluation of spin-triplet*
206 *superconductivity in Sr_2RuO_4* , *Journal of the Physical Society of Japan* **81**(1), 011009
207 (2011), doi:[10.1143/JPSJ.81.011009](https://doi.org/10.1143/JPSJ.81.011009).
- 208 [4] C. Kallin and A. J. Berlinsky, *Is Sr_2RuO_4 a chiral p-wave superconductor?*, *J. Physics:*
209 *Cond. Mat.* **21**(16), 164210 (2009), doi:[10.1088/0953-8984/21/16/164210](https://doi.org/10.1088/0953-8984/21/16/164210).
- 210 [5] C. Kallin, *Chiral p-wave order in Sr_2RuO_4* , *Rep. Progr. Phys.* **75**, 042501 (2012),
211 doi:[10.1088/0034-4885/75/4/042501](https://doi.org/10.1088/0034-4885/75/4/042501).
- 212 [6] R. Joynt and L. Taillefer, *The superconducting phases of UPt_3* , *Reviews of Modern Physics*
213 **74**(1), 235 (2002), doi:[10.1103/RevModPhys.74.235](https://doi.org/10.1103/RevModPhys.74.235).
- 214 [7] F. Yuqiang, J. Pan, D. Zhang, D. Wang, H. Hirose, T. Terashima, S. Uji, Y. Yuan, W. Li,
215 Z. Tian, J. Xue, Y. Ma *et al.*, *Discovery of Superconductivity in 2M WS_2 with Possible Topo-*
216 *logical Surface States*, *Adv. Mater.* p. 1901942 (2019), doi:[10.1002/adma.201901942](https://doi.org/10.1002/adma.201901942).
- 217 [8] L. Fu and E. Berg, *Odd-Parity Topological Superconductors: Theory and Application to*
218 *$Cu_xBi_2Se_3$* , *Phys. Rev. Lett.* **105**, 097001 (2010), doi:[10.1103/PhysRevLett.105.097001](https://doi.org/10.1103/PhysRevLett.105.097001).
- 219 [9] Y. S. Hor, A. J. Williams, J. G. Checkelsky, P. Roushan, J. Seo, Q. Xu, H. W. Zandbergen,
220 A. Yazdani, N. P. Ong and R. J. Cava, *Superconductivity in $Cu_xBi_2Se_3$ and its Implications*
221 *for Pairing in the Undoped Topological Insulator*, *Phys. Rev. Lett.* **104**, 057001 (2010),
222 doi:[10.1103/PhysRevLett.104.057001](https://doi.org/10.1103/PhysRevLett.104.057001).
- 223 [10] W. Zhu, R. Song, J. Huang, Q.-W. Wang, Y. Cao, R. Zhai, Q. Bian, Z. Shao, H. Jing, L. Zhu
224 *et al.*, *Intrinsic surface p-wave superconductivity in layered $AuSn_4$* , *Nature Communications*
225 **14**(1), 7012 (2023), doi:[10.1038/s41467-023-42781-7](https://doi.org/10.1038/s41467-023-42781-7).
- 226 [11] D. Shen, C. N. Kuo, T. W. Yang, I. N. Chen, C. S. Lue and L. M. Wang, *Two-dimensional su-*
227 *perconductivity and magnetotransport from topological surface states in $AuSn_4$ semimetal*,
228 *Communications Materials* **1**(1), 56 (2020), doi:[10.1038/s43246-020-00060-8](https://doi.org/10.1038/s43246-020-00060-8).
- 229 [12] N. Karn, M. Sharma and V. Awana, *Non-trivial band topology in the superconductor $AuSn_4$:*
230 *a first principle study*, *Superconductor Science and Technology* **35**(11), 114002 (2022),
231 doi:[10.1088/1361-6668/ac9160](https://doi.org/10.1088/1361-6668/ac9160).
- 232 [13] E. Herrera, B. Wu, E. O’Leary, A. M. Ruiz, M. Águeda, P. G. Talavera, V. Barrena,
233 J. Azpeitia, C. Munuera, M. García-Hernández *et al.*, *Band structure, superconduc-*
234 *tivity, and polytypism in $AuSn_4$* , *Physical Review Materials* **7**(2), 024804 (2023),
235 doi:[10.1103/PhysRevMaterials.7.024804](https://doi.org/10.1103/PhysRevMaterials.7.024804).
- 236 [14] M. Gendron and R. Jones, *Superconductivity in the $CuAl_2$ ($C16$) crystal class*, *J. Phys.*
237 *Chem. Sol.* **23**(4), 405 (1962), doi:[10.1016/0022-3697\(62\)90107-5](https://doi.org/10.1016/0022-3697(62)90107-5).
- 238 [15] Y. Wu, L.-L. Wang, E. Mun, D. D. Johnson, D. Mou, L. Huang, Y. Lee, S. L. Bud’ko, P. C.
239 Canfield and A. Kaminski, *Dirac node arcs in $PtSn_4$* , *Nature Physics* **12**(7), 667 (2016),
240 doi:[10.1038/nphys3712](https://doi.org/10.1038/nphys3712).

- 241 [16] N. H. Jo, Y. Wu, L.-L. Wang, P. P. Orth, S. S. Downing, S. Manni, D. Mou, D. D. John-
242 son, A. Kaminski, S. L. Bud'ko *et al.*, *Extremely large magnetoresistance and Kohler's rule*
243 *in PdSn₄: A complete study of thermodynamic, transport, and band-structure properties*,
244 *Physical Review B* **96**(16), 165145 (2017), doi:[10.1103/PhysRevB.96.165145](https://doi.org/10.1103/PhysRevB.96.165145).
- 245 [17] M. Sharma, G. Gurjar, S. Patnaik and V. Awana, *Two-fold anisotropic superconducting*
246 *state in topological superconductor Sn₄Au*, *Europhysics Letters* **142**(2), 26004 (2023),
247 doi:[10.1209/0295-5075/acc8f5](https://doi.org/10.1209/0295-5075/acc8f5).
- 248 [18] J. Bardeen, L. N. Cooper and J. R. Schrieffer, *Microscopic theory of superconductivity*,
249 *Phys. Rev.* **106**(1), 162 (1957), doi:[10.1103/physrev.106.162](https://doi.org/10.1103/physrev.106.162).
- 250 [19] J. Bardeen, L. N. Cooper and J. R. Schrieffer, *Theory of Superconductivity*, *Phys. Rev.* **108**,
251 1175 (1957), doi:[10.1103/PhysRev.108.1175](https://doi.org/10.1103/PhysRev.108.1175).
- 252 [20] H. Okamoto, *Au-Sn (gold-tin)*, *Journal of phase equilibria* **14**(6), 765 (1993),
253 doi:[10.1007/s11669-007-9147-1](https://doi.org/10.1007/s11669-007-9147-1).
- 254 [21] P. C. Canfield, *New materials physics*, *Reports on Progress in Physics* **83**(1), 016501
255 (2019), doi:[10.1088/1361-6633/ab514b](https://doi.org/10.1088/1361-6633/ab514b).
- 256 [22] C. T. Van Degrift, *Tunnel diode oscillator for 0.001 ppm measurements at low temperatures*,
257 *Review of Scientific Instruments* **46**(5), 599 (1975), doi:[10.1063/1.1134272](https://doi.org/10.1063/1.1134272).
- 258 [23] R. Prozorov, R. W. Giannetta, A. Carrington and F. M. Araujo-Moreira, *Meissner-london*
259 *state in superconductors of rectangular cross section in a perpendicular magnetic field*, *Phys.*
260 *Rev. B* **62**, 115 (2000), doi:[10.1103/PhysRevB.62.115](https://doi.org/10.1103/PhysRevB.62.115).
- 261 [24] R. Prozorov, R. W. Giannetta, A. Carrington, P. Fournier, R. L. Greene, P. Guptasarma,
262 D. G. Hinks and A. R. Banks, *Measurements of the absolute value of the penetration depth*
263 *in high-T_c superconductors using a low-T_c superconductive coating*, *Appl. Phys. Lett.* **77**,
264 4202 (2000), doi:[10.1063/1.1328362](https://doi.org/10.1063/1.1328362).
- 265 [25] R. Prozorov, *Meissner-london susceptibility of superconducting right circular cylin-*
266 *ders in an axial magnetic field*, *Phys. Rev. App.* **16**(2), 024014 (2021),
267 doi:[10.1103/physrevapplied.16.024014](https://doi.org/10.1103/physrevapplied.16.024014).
- 268 [26] R. Giannetta, A. Carrington and R. Prozorov, *London Penetration Depth Measure-*
269 *ments Using Tunnel Diode Resonators*, *J. Low Temp. Phys.* **208**(1-2), 119 (2022),
270 doi:[10.1007/s10909-021-02626-3](https://doi.org/10.1007/s10909-021-02626-3).
- 271 [27] A. C. Damask and G. J. Dienes, *Point Defects in Metals*, Gordon & Breach Science Pub-
272 lishers Ltd, ISBN 0677001908 (1963).
- 273 [28] M. W. Thompson, *Defects and Radiation Damage in Metals*, Cambridge Monographs
274 on Physics. Cambridge University Press, revised september 27, 1974 edn., ISBN
275 0521098653 (1969).
- 276 [29] R. Prozorov, M. Kończykowski, M. A. Tanatar, A. Thaler, S. L. Bud'ko, P. C. Canfield,
277 V. Mishra and P. J. Hirschfeld, *Effect of Electron Irradiation on Superconductivity in*
278 *Single Crystals of Ba(Fe_{1-x}Ru_x)₂As₂ (x = 0.24)*, *Phys. Rev. X* **4**, 041032 (2014),
279 doi:[10.1103/PhysRevX.4.041032](https://doi.org/10.1103/PhysRevX.4.041032).
- 280 [30] R. Prozorov, M. Kończykowski, M. A. Tanatar, H.-H. Wen, R. M. Fernandes and P. C.
281 Canfield, *Interplay between superconductivity and itinerant magnetism in underdoped*
282 *Ba_{1-x}K_xFe₂As₂ (x=0.2) probed by the response to controlled point-like disorder*, *npj Quan-*
283 *tum Materials* **4**(1), 34 (2019), doi:[10.1038/s41535-019-0171-2](https://doi.org/10.1038/s41535-019-0171-2).

- 284 [31] M. Tinkham, *Introduction to Superconductivity*, Dover Publications, 2 edn., ISBN
285 0486435032 (2004).
- 286 [32] V. Kogan, R. Prozorov and V. Mishra, *London penetration depth and pair breaking*, Phys.
287 Rev. B **88**(22), 224508 (2013), doi:[10.1103/PhysRevB.88.224508](https://doi.org/10.1103/PhysRevB.88.224508).
- 288 [33] R. T. Gordon, N. Ni, C. Martin, M. A. Tanatar, M. D. Vannette, H. Kim, G. D. Samolyuk,
289 J. Schmalian, S. Nandi, A. Kreyssig, A. I. Goldman, J. Q. Yan *et al.*, *Unconventional*
290 *London Penetration Depth in Single-Crystal $\text{Ba}(\text{Fe}_{0.93}\text{Co}_{0.07})_2\text{As}_2$ Superconductors*, Phys.
291 Rev. Lett. **102**, 127004 (2009), doi:[10.1103/PhysRevLett.102.127004](https://doi.org/10.1103/PhysRevLett.102.127004).
- 292 [34] H. Kim, M. A. Tanatar, Y. J. Song, Y. S. Kwon and R. Prozorov, *Nodeless two-gap supercon-*
293 *ducting state in single crystals of the stoichiometric iron pnictide LiFeAs* , Phys. Rev. B **83**,
294 100502 (2011), doi:[10.1103/PhysRevB.83.100502](https://doi.org/10.1103/PhysRevB.83.100502).
- 295 [35] E. I. Timmons, S. Teknowijoyo, M. Kończykowski, O. Cavani, M. A. Tanatar, S. Ghimire,
296 K. Cho, Y. Lee, L. Ke, N. H. Jo, S. L. Bud'ko, P. C. Canfield *et al.*, *Electron irradiation effects*
297 *on superconductivity in PdTe_2 : An application of a generalized Anderson theorem*, Phys.
298 Rev. Res. **2**(2), 023140 (2020), doi:[10.1103/PhysRevResearch.2.023140](https://doi.org/10.1103/PhysRevResearch.2.023140).
- 299 [36] P. W. Anderson, *Theory of dirty superconductors*, Journal of Physics and Chemistry of
300 Solids **11**(1-2), 26 (1959), doi:[Doi: 10.1016/0022-3697\(59\)90036-8](https://doi.org/10.1016/0022-3697(59)90036-8).
- 301 [37] S. Ghimire, K. R. Joshi, E. H. Krenkel, M. A. Tanatar, Y. Shi, M. Kończykowski, R. Gras-
302 set, V. Taufour, P. P. Orth, M. S. Scheurer and R. Prozorov, *Electron irradiation reveals*
303 *robust fully gapped superconductivity in LaNiGa_2* , Phys. Rev. B **109**, 024515 (2024),
304 doi:[10.1103/PhysRevB.109.024515](https://doi.org/10.1103/PhysRevB.109.024515).
- 305 [38] V. G. Kogan, *Homes scaling and BCS*, Phys. Rev. B **87**, 220507 (2013),
306 doi:[10.1103/PhysRevB.87.220507](https://doi.org/10.1103/PhysRevB.87.220507).
- 307 [39] G. Eilenberger, *Transformation of Gorkov's equation for type II superconductors into*
308 *transport-like equations*, Zeitschrift für Physik A Hadrons and nuclei **214**, 195 (1968),
309 doi:[10.1007/BF01379803](https://doi.org/10.1007/BF01379803).
- 310 [40] A. M. Campbell, *The response of pinned flux vortices to low-frequency fields*, Journal of
311 Physics C: Solid State Physics **2**(8), 1492 (1969), doi:[10.1088/0022-3719/2/8/318](https://doi.org/10.1088/0022-3719/2/8/318).
- 312 [41] A. M. Campbell, *The interaction distance between flux lines and pinning centres*, Journal of
313 Physics C: Solid State Physics **4**(18), 3186 (1971), doi:[10.1088/0022-3719/4/18/023](https://doi.org/10.1088/0022-3719/4/18/023).
- 314 [42] R. Willa, V. B. Geshkenbein and G. Blatter, *Campbell penetration in the critical state of type-*
315 *II superconductors*, Phys. Rev. B **92**, 134501 (2015), doi:[10.1103/PhysRevB.92.134501](https://doi.org/10.1103/PhysRevB.92.134501).
- 316 [43] F. Gaggioli, G. Blatter and V. B. Geshkenbein, *Creep effects on the Camp-*
317 *bell response in type-II superconductors*, Phys. Rev. Res. **4**, 013143 (2022),
318 doi:[10.1103/PhysRevResearch.4.013143](https://doi.org/10.1103/PhysRevResearch.4.013143).
- 319 [44] E. H. Brandt, *Penetration of magnetic ac fields into type-II superconductors*, Phys. Rev. Lett.
320 **67**, 2219 (1991), doi:[10.1103/PhysRevLett.67.2219](https://doi.org/10.1103/PhysRevLett.67.2219).
- 321 [45] A. E. Koshelev and V. M. Vinokur, *Frequency response of pinned vortex lattice*, Physica C
322 **173**, 465 (1991), doi:[10.1016/0921-4534\(91\)90749-o](https://doi.org/10.1016/0921-4534(91)90749-o).
- 323 [46] R. Prozorov, R. W. Giannetta, N. Kameda, T. Tamegai, J. A. Schlueter and P. Fournier,
324 *Campbell penetration depth of a superconductor in the critical state*, Phys. Rev. B **67**(18),
325 184501 (2003), doi:[10.1103/PhysRevB.67.184501](https://doi.org/10.1103/PhysRevB.67.184501).

- 326 [47] G. Ghigo, D. Torsello, L. Gozzelino, M. Fracasso, M. Bartoli, C. Pira, D. Ford, G. Mar-
327 conato, M. Fretto, I. De Carlo, N. Pompeo and E. Silva, *Vortex dynamics in NbTi*
328 *films at high frequency and high DC magnetic fields*, Sci. Rep. **13**(1), 1 (2023),
329 doi:[10.1038/s41598-023-36473-x](https://doi.org/10.1038/s41598-023-36473-x).
- 330 [48] H. Kim, M. A. Tanatar, H. Hodovanets, K. Wang, J. Paglione and R. Prozorov, *Campbell*
331 *penetration depth in low carrier density superconductor YPtBi*, Phys. Rev. B **104**, 014510
332 (2021), doi:[10.1103/PhysRevB.104.014510](https://doi.org/10.1103/PhysRevB.104.014510).
- 333 [49] J. Srpčić, M. Ainslie, Y. Shi and J. Durrell, *The Campbell penetration depth in type-II super-*
334 *conductors*, In *7th International Workshop on Numerical Modelling of High Temperature*
335 *Superconductors (HTS 2020)* (2021).
- 336 [50] S. Ghimire, F. Gaggioli, K. R. Joshi, M. Konczykowski, R. Grasset, E. H. Krenkel,
337 A. Datta, M. A. Tanatar, S. Chen, C. Petrovic, V. B. Geshkenbein and R. Prozorov, *Non-*
338 *monotonic relaxation of Campbell penetration depth from creep-enhanced vortex pinning*,
339 arXiv:2403.14891 (2024), doi:[10.48550/arXiv.2403.14891](https://doi.org/10.48550/arXiv.2403.14891).
- 340 [51] R. Gordon, N. Zhigadlo, S. Weyeneth, S. Katrych and R. Prozorov, *Conventional supercon-*
341 *ductivity and hysteretic Campbell penetration depth in single crystals MgCNi₃*, Phys. Rev.
342 B **87**(9), 094520 (2013), doi:[10.1103/PhysRevB.87.094520](https://doi.org/10.1103/PhysRevB.87.094520).
- 343 [52] R. Willa, V. B. Geshkenbein, R. Prozorov and G. Blatter, *Campbell response in type-II*
344 *superconductors under strong pinning conditions*, Phys. Rev. Lett. **115**, 207001 (2015),
345 doi:[10.1103/PhysRevLett.115.207001](https://doi.org/10.1103/PhysRevLett.115.207001).
- 346 [53] G. Blatter, M. V. Feigel'man, V. B. Geshkenbein, A. I. Larkin and V. M. Vinokur,
347 *Vortices in high-temperature superconductors*, Rev. Mod. Phys. **66**, 1125 (1994),
348 doi:[10.1103/RevModPhys.66.1125](https://doi.org/10.1103/RevModPhys.66.1125).
- 349 [54] R. Prozorov, V. G. Kogan, M. D. Vannette, S. L. Bud'ko and P. C. Canfield,
350 *Radio-frequency magnetic response of vortex lattices undergoing structural transforma-*
351 *tions in superconducting borocarbide crystals*, Phys. Rev. B **76**, 094520 (2007),
352 doi:[10.1103/PhysRevB.76.094520](https://doi.org/10.1103/PhysRevB.76.094520).